

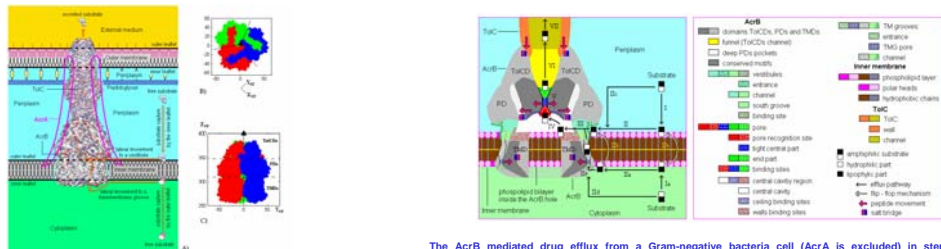
Quantitative Drug Structure – Complex Geometry Relationships in β -Lactam Efflux by Bacterial Multidrug Resistance Pump AcrAB-ToIC

Márcia Miguel Castro Ferreira and Rudolf Kiralj. marcia@iqm.unicamp.br, rudolf@iqm.unicamp.br, <http://lqta.iqm.unicamp.br>
 Laboratório de Quimiometria Teórica e Aplicada (LQTA), Instituto de Química, Universidade Estadual de Campinas, Campinas SP, 13084-971, Brazil

THE PRIMARY OBJECTIVES OF THIS WORK

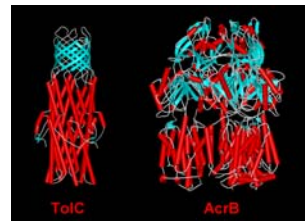
- 1) To predict position and orientation of 16 β -lactam antibiotics in the central cavity of the multidrug efflux pump AcrB (a component of AcrAB-ToIC membrane transporter) that exists in several Gram-negative bacteria \rightarrow using only known molecular structures and calculated properties of drugs (β -lactams and four organic dyes: dequalinium, ethidium, ciprofloxacin, rhodamine 6G) and protein-drug (AcrB-organic dyes) complexes \rightarrow no protein-drug complex geometry optimizations nor molecular dynamics simulations were performed;
- 2) To show that the β -lactams and the organic dyes, although structurally diverse, have properties in common that are responsible for their active efflux;
- 3) To use this similarity and the AcrB-organic dye complexes to predict AcrB- β -lactam geometry \rightarrow Quantitative Drug Structure – Complex Geometry Relationships.

BACTERIAL MULTIDRUG RESISTANCE VIA ACTIVE DRUG EFFLUX BY MEANS OF A PROTON-DEPENDENT AcrAB-ToIC PUMP

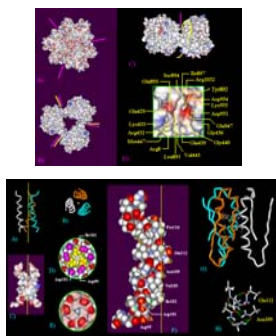


A): Combined 3D - schematic representation of AcrAB-ToIC pump in *E. coli*. Two main drug efflux mechanism are shown, one starting in the periplasm, and other in the cytoplasm. B) and C): Blue, red and green AcrB protomers around the symmetry axis.

The AcrB mediated drug efflux from a Gram-negative bacteria cell (AcrA is excluded) in steps 1 - VII. Hydrophilic/lipophilic orientation of an amphiphilic drug is also visible. Conserved motifs, salt bridges and principal peptide movements are marked with special symbols. The efflux mechanism consists of a series of allosteric effects initiated by proton influx, braking of salt bridges and hydrogen bonds, changing of pump conformation and opening its efflux channel components, binding drugs in the central cavity and extruding them through the pore and ToIC.



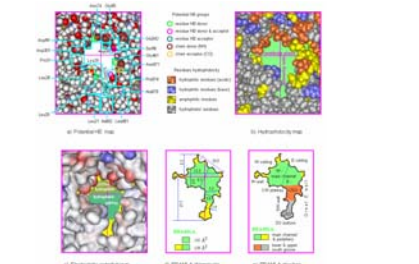
Schematic representation of the 3D structure of trimmer ToIC (PDB: 1EK9, space group R3. V. Koronakis *et al.*, *Nature* 305, 2000, 914) and AcrB (PDB: 1IWG, space group R32. S. Murakami *et al.*, *Nature* 419, 2002, 587) showing α -helices, β -sheets and coils.



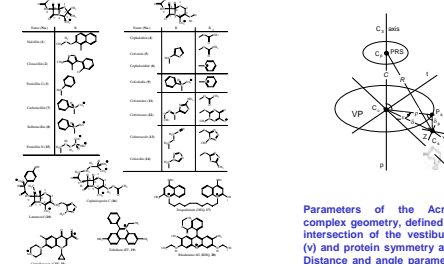
Electrostatic potential of the A) pore domains (PDs) and B) transmembrane domains (TMDs) viewed upwards and downwards the vestibule plane, respectively. C) The transmembrane groove (TMG) circular shape and position at the TMDs surface. The position of the vestibules (pink line) and the TMGs (yellow circle). D) The TMG pore at its entrance, with essential residues.

The pore channel viewed perpendicularly to A) and along with B) the symmetry axis. C) The pore channel interior excluding a pore helix. The pore recognition site represented by CPK model (D) and electrostatic potential (E). F) A pore helix from a promoter represented by CPK model and hydrogen bond donor (Ds) and acceptor (As) groups from residues (yellow) and the polypeptide chain (green). G) Three RND conserved motifs including the pore with hydrogen bonding residues that keep the pore to be tight. H) These residues with their hydrogen bond network.

ESSENTIALS OF THE RECEPTOR, SUBSTRATE AND COMPLEX STRUCTURE



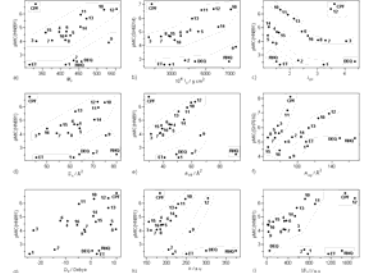
Vestibule and its 2D representation BRAMLA (BRAZIL Map-Like Area). a) Potential hydrogen bonding groups from residues and polypeptide chains. b) The hydrophobic character of the residues. c) The electrostatic potential map. d) BRAMLA area with its dimensions (d) and regions of its interior and exterior (E).



Chemical structures of studied AcrB-ToIC substrates: β -lactam antibiotics (1-16) with atomic numbering dequalinium (17), ciprofloxacin (18), ethidium (19) and rhodamine 6G (20).

Parameters of the AcrB-drug complex geometry, defined by the intersection of the vestibule axis (V) and protein symmetry axis (p). Distance and angle parameters of the drug are dependent variables that are quantitatively related to several steric and electronic molecular descriptors of 1-20.

PREDICTION OF β -LACTAM POSITION AND ORIENTATION IN THE CENTRAL CAVITY OF AcrB

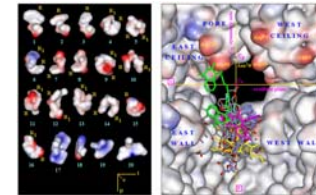


Representative efflux activity-drug molecular descriptor plots important for elucidation of the efflux mechanism: a) pMIC(HN891) - A_{10} ; b) pMIC(SH5014) - L_1 ; c) pMIC(HN891) - L_2 ; d) pMIC(HN891) - S_1 ; e) pMIC(SH5014) - A_1 ; f) pMIC(SH7616) - A_{10} ; g) pMIC(HN891) - D_2 ; h) pMIC(HN891) - α_1 ; i) pMIC(HN891) - β_1 . See the next Table for definition of molecular descriptors that were calculated in this and previous work (M. M. C. Ferreira, R. Kiralj, *J. Chemometr.*, 18, 2004, 242-252).

Symbol	Linear and description	Linear ^a	log ₁₀	log ₁₀ ^b	log ₁₀ ^c
A_{10}	radius molecular mass	steric	conjug	po	tw
A_{11}	1st principal moment of inertia (around axis Z)	steric	conjug	po	tw
A_{12}	2nd principal moment of inertia (around axis Y)	steric	conjug	po	tw
A_{13}	3rd principal moment of inertia (around axis X)	steric	conjug	po	tw
A_{14}	ratio between the principal moments A_{11}/A_{12}	steric	conjug	po	tw
A_{15}	ratio between the principal moments A_{11}/A_{13}	steric	conjug	po	tw
A_{16}	ratio between the principal moments A_{12}/A_{13}	steric	conjug	po	tw
A_{17}	molecular area projected on the YZ plane (along X axis, in the CPK molecular model)	steric	conjug	po	tw
A_{18}	area of the XY face of the molecule box defined by the CPK molecular model	steric	conjug	po	tw
A_{19}	molecular polarizability	electronic	conjug	po	tw
A_{20}	absolute 3rd-order molecular polarizability β	electronic	conjug	po	tw
A_{21}	absolute X component of β	electronic	conjug	po	tw
A_{22}	absolute Y component of β	electronic	conjug	po	tw
A_{23}	X component of molecular dipole moment	electronic	conjug	po	tw
A_{24}	Y component of molecular dipole moment	electronic	conjug	po	tw
A_{25}	Z component of molecular dipole moment	electronic	conjug	po	tw
A_{26}	surface molecular density projected on the YZ plane, defined as N/A_{17} , where N is the number of atoms	steric	conjug	po	tw
A_{27}	the length of the molecule box along the axis X in the CPK molecular model	steric	conjug	po	tw
A_{28}	the width(Y/Z)axis/2 ratio (of the YZ face of the molecule box in the CPK molecular model)	steric	conjug	po	tw
A_{29}	area of the XY face of the molecule box defined by the maximum and minimum atomic coordinates	steric	conjug	po	tw
A_{30}	area of the YZ face of the molecule box defined by the maximum and minimum atomic coordinates	steric	conjug	po	tw
A_{31}	area of the XZ face of the molecule box defined by the maximum and minimum atomic coordinates	steric	conjug	po	tw
A_{32}	ratio between the X and Y difference	steric	conjug	po	tw
A_{33}	ratio between the X and Z difference	steric	conjug	po	tw
A_{34}	ratio between the Y and Z difference	steric	conjug	po	tw
A_{35}	difference between the maximum and minimum of (Y coordinate + α Y radius)	steric	conjug	po	tw
A_{36}	difference between the β_{10} and β_{11} difference	steric	conjug	po	tw
A_{37}	area of the XY face of the molecule box defined by the maximum and minimum atomic coordinates	steric	conjug	po	tw
A_{38}	area of the YZ face of the molecule box defined by the maximum and minimum atomic coordinates	steric	conjug	po	tw
A_{39}	area of the XZ face of the molecule box defined by the maximum and minimum atomic coordinates	steric	conjug	po	tw
A_{40}	ratio between the X and Y difference	steric	conjug	po	tw
A_{41}	ratio between the X and Z difference	steric	conjug	po	tw
A_{42}	ratio between the Y and Z difference	steric	conjug	po	tw
A_{43}	difference between the maximum and minimum of (Y coordinate + α Y radius)	steric	conjug	po	tw

Experimental and predicted AcrB - substrate geometry

Phenotype	Experimental (for 17-20)			Predicted (for β -lactams 1-16)		
	DEQ	CPF	ET	RHQ	Molecular descriptors	range
CPX	7.08	6.20	7.38	7.08	$^{16}A_{10} \cdot A_{11} \cdot A_{12}$	6.8-9.7
ϕ_1/A	2.64	7.20	8.20	15.02	$^{16}A_{10} \cdot 10^5$	6.5-14.0
ϕ_2/A	4.48	13.00	5.00	8.55	$^{16}A_{10} \cdot \beta_1 \cdot \beta_2 \cdot \beta_3 \cdot \beta_4 \cdot \beta_5$	7.6-9.7
β/A	5.20	14.94	9.74	17.29	$^{16}A_{10} \cdot 10^5$	10.0-17.1
β_1/A	10.00	10.00	10.00	23.91	$^{16}A_{10} \cdot 10^5$	10.4-23.1
A_{10}	82.9	70.0	80.0	87.0	$^{16}A_{10}$	87-100
A_{11}	70.0	140.0	70.0	99.0	$^{16}A_{11}$	70-150
A_{12}	160.0	65.0	19.0	9.0	$^{16}A_{12}$	0-150
A_{13}	151.0	108.0	82.0	99.0	$^{16}A_{13}$	82-100
A_{14}	118.0	110.0	19.0	160.0	$^{16}A_{14} \cdot A_{10} \cdot A_{11} \cdot A_{12}$	77-100
A_{15}	100.0	94.0	70.0	99.0	$^{16}A_{15}$	149-180
A_{16}	78.0	4.0	10.0	1.0	$^{16}A_{16} \cdot A_{10} \cdot A_{11} \cdot A_{12}$	83-99
Δ_{10}	15.0	77.0	168.0	171.0	$^{16}A_{10} \cdot A_{11} \cdot A_{12}$	44-162
Δ_{11}	116.0	111.0	80.0	82.0	$^{16}A_{11} \cdot A_{10}$	77-110
Δ_{12}	100.0	155.0	80.0	80.0	$^{16}A_{12} \cdot A_{10} \cdot A_{11}$	70-140
Δ_{13}	100.0	21.0	80.0	80.0	$^{16}A_{13} \cdot A_{10}$	54-115



a) Electrostatic potential of 1-20. Most drugs expose positive, amphiphilic or hydrophobic heads (R or R₁) toward predominantly negatively charged ceiling and the pore. b) 16 β -lactams in predicted position/orientation in the central cavity, with experimental location of DEQ (green), CPF (light blue), ET (pink) and RHQ (yellow). Important charged residues are labeled at the pore region. Linear relationships between the dependent variables (protein-drug complex geometry parameters) and various electronic (dipole moment components, polarizabilities) and steric (principal moments of inertia and their ratios, molecular box size parameters) molecular descriptors of drugs 17-20 were established. These relationships were then used to predict the orientational/positional parameters for β -lactams.

Experimental and predicted values of the dependent variables for the four drugs (DEQ, CPF, ET, RHQ) and β -lactams (1-16), respectively.